JOURNAL OF THE MECHANICAL BEHAVIOR OF BIOMEDICAL MATERIALS 59 (2016) 241–250

Available online at www.sciencedirect.com

ScienceDirect

www.elsevier.com/locate/jmbbm

Research paper

Numerical investigation of the mechanical properties of the additive manufactured bone scaffolds fabricated by FDM: The effect of layer penetration and post-heating

S. Naghieh[a], M.R. Karamooz Ravari[b], M. Badrossamay[a], E. Foroozmehr[a,*], M. Kadkhodaei[a]

[a]Department of Mechanical Engineering, Isfahan University of Technology, 84156-83111 Isfahan, Iran
[b]Department of Mechanical Engineering, Graduate University of Advanced Technology, 76311-33131 Kerman, Iran

ARTICLE INFO

Article history:
Received 12 November 2015
Received in revised form
25 January 2016
Accepted 27 January 2016
Available online 4 February 2016

Keywords:
Additive manufacturing
Fused deposition modeling
Bone scaffolds
Mechanical response
Finite element analysis
Elastic modulus

ABSTRACT

In recent years, thanks to additive manufacturing technology, researchers have gone towards the optimization of bone scaffolds for the bone reconstruction. Bone scaffolds should have appropriate biological as well as mechanical properties in order to play a decisive role in bone healing. Since the fabrication of scaffolds is time consuming and expensive, numerical methods are often utilized to simulate their mechanical properties in order to find a nearly optimum one. Finite element analysis is one of the most common numerical methods that is used in this regard. In this paper, a parametric finite element model is developed to assess the effects of layers penetration's effect on inter-layer adhesion, which is reflected on the mechanical properties of bone scaffolds. To be able to validate this model, some compression test specimens as well as bone scaffolds are fabricated with biocompatible and biodegradable poly lactic acid using fused deposition modeling. All these specimens are tested in compression and their elastic modulus is obtained. Using the material parameters of the compression test specimens, the finite element analysis of the bone scaffold is performed. The obtained elastic modulus is compared with experiment indicating a good agreement. Accordingly, the proposed finite element model is able to predict the mechanical behavior of fabricated bone scaffolds accurately. In addition, the effect of post-heating of bone scaffolds on their elastic modulus is investigated. The results demonstrate that the numerically predicted elastic modulus of scaffold is closer to experimental outcomes in comparison with as-built samples.

© 2016 Elsevier Ltd. All rights reserved.

*Corresponding author.
E-mail address: eforoozmehr@cc.iut.ac.ir (E. Foroozmehr).

http://dx.doi.org/10.1016/j.jmbbm.2016.01.031
1751-6161/© 2016 Elsevier Ltd. All rights reserved.

1. Introduction

Tissue engineering is "an interdisciplinary field that bring the principles of engineering and life sciences together to develop biological substitutes in order to restore, maintain, or improve tissue function or a whole organ" (Godbey and Atala, 2002). Although treatment methods like allograft and autograft are the gold standard for treatment of some diseases and tumors, they have undeniable deficiencies. As an example, fracture, non-union and infection are some complicated drawbacks of more than 30% of the allograft procedures and also requiring high volume of bone in autograft method (De Long et al., 2007; Doyle et al., 2015). Therefore, researchers have gone toward preparation of suitable structural frameworks named bone scaffold to provide a support for cells (Jariwala et al., 2015; Poh, 2014). Such structures should have appropriate geometrical and mechanical properties in order to provide suitable bone treatment (Giannitelli et al., 2014; Sanz-Herrera et al., 2008; Yang et al., 2001). In this regard, Dias et al. (2014) proposed a topology optimization algorithm for designing scaffolds that satisfy both mass transport and mechanical load bearing capacity.

In addition to the desirable shape for defected site, bone scaffolds should have enough porosity and pore interconnectivity to provide the possibility of cell ingrowth and nutrition exchange (Brown, 2000; Hollister and Lin, 2007; Mullender et al., 2004). In addition, the base material's properties such as biocompatibility and bioresorbability are of vital Importance for the design of bone scaffolds. Furthermore, a bone scaffold should have appropriate surface chemistry and adequate mechanical properties with respect to its applications (Hutmacher, 2000). Until now, both synthetic and natural polymers have been studied as scaffolds for bone tissue engineering applications (Singh et al., 2015). The results of these investigations show that a polymer-based scaffold should have a three-dimensional porous matrix.

There are various processing methods for producing bone scaffolds (Widmer and Mikos, 1998) from conventional ones like phase separation (Gao et al., 2003), emulsion freeze-drying (Whang et al., 1995), gas foaming (Harris et al., 1998), fiber templates (Thomson et al., 1995) and porogen leaching (Mikos et al., 1993; Zhou et al., 2005) to additive manufacturing (AM) techniques (Hutmacher, 2000; Moroni et al., 2006). Over the past decades, due to the possibility of fabricating complex microstructures with controllable pore shape and size, AM techniques have been widely utilized for fabrication of bone scaffolds. In fact, these techniques are able to eliminate various drawbacks of conventional methods, e.g. uncontrollable structure.

AM techniques are divided into seven categories including powder bed fusion, extrusion-based, material jetting, binder jetting, sheet lamination, directed energy deposition and vat photopolymerization processes (Gibson et al., 2015). Fused deposition modeling (FDM), which is based on depositing a thread of molten thermoplastic material onto a substrate, is a low cost extrusion based AM technique. In addition to various significant benefits, like lack of any need to solvent, FDM presents unique features of ease and flexibility in material selection, processing and simplicity of fabrication process. Also, using from materials in filament shape allows nonstop production without consuming any time for replacing feedstock (Zein et al., 2002). A schematic of FDM process is shown in Fig. 1.

Although FDM has become more and more popular in the last decade, fabrication of numerous compressive specimens as well as bone scaffolds is really time-consuming causing it to not be economically recommended. Accordingly, finite element method (FEM) is used to overcome this deficiency by predicting the mechanical response of FDM parts before fabrication (Martínez et al., 2013) causing the reduction of the final fabrication cost by decreasing the required experimental measurements (Liu and Zheng, 2010). Also, if the mechanical behavior of bulk material of tissue scaffolds is identified, then with the assistance of FEM, it is possible to predict the behavior of complex formations such as mechanical response at microscopic level during the cell differentiation (Sahai et al., 2016).

There are several studies in the literature which are concentrated on the numerical analysis of bone scaffolds, especially using the finite element method. This method has been utilized effectively for the prediction of mechanical properties of additive manufactured scaffolds (Giannitelli et al., 2014). Boccaccio et al. (2011) developed computational mechno-regulation models for determining porosity as well as structural response of scaffolds during the time. Wieding et al. (2014) optimized the geometrical parameters of porous scaffolds to match the elastic modulus of human cortical bone. Laurent et al. (2014) proposed a finite element model for predicting the geometrical evolution of a biodegradable polymer scaffold for ligament tissue engineering. FEM is also used to predict the mechanical response of bone scaffolds as well as cellular lattices structures (Karamooz Ravari and Kadkhodaei, 2015, 2013; Karamooz Ravari et al., 2015a, 2015b, 2014). The results of these investigations show a good

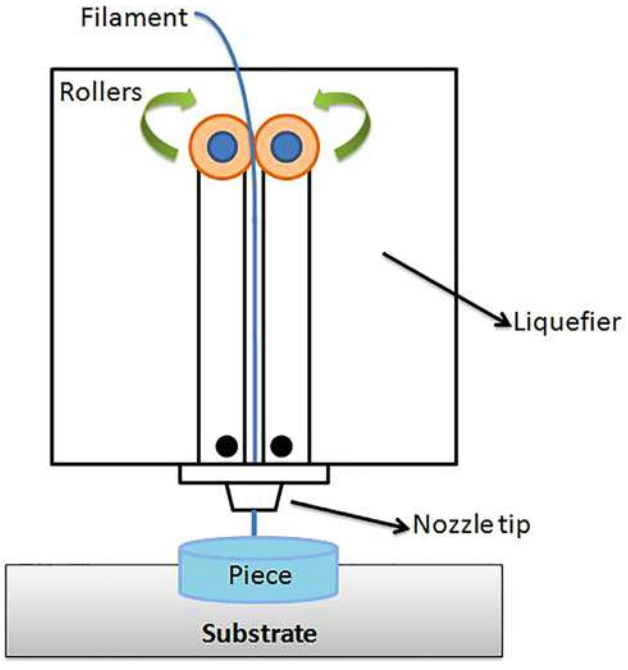

Fig. 1 – Schematic diagram of the FDM machine.

agreement with those obtained from experimental measurements. Apart from FEM in literature, there are plenty of studies on the experimental work in this area. Sudarmadji et al. (2011) fabricated polymeric tissue scaffolds with various structures as well as porosity values implementing selective laser sintering technique. They reported the stress–strain curves of the performed compression tests and showed that the stiffness of the fabricated scaffolds matched with the properties of the cancellous bone. Additionally, Scaffaro et al. (2016) reported that pore architecture has a paramount effect on the mechanical properties by performing various compression tests. Ang et al. (2007) studied the fabrication of PCL/HA composites as a structure which could be used in tissue engineering. They reported that the obtained composition had improved compressive properties comparing with the polymeric structures fabricated by PCL.

The main goal of this study is to develop a finite element model for predicting the elastic mechanical response of porous polymeric bone scaffolds fabricated by fused deposition modeling process. Hence, some bone scaffolds are fabricated by FDM technique using appropriate geometrical parameters reported in the literature. For this purpose, a specialized program is developed as a G-Code for the fabrication of bone scaffolds via FDM machine. To be able to characterize the bulk material of the bone scaffolds for modeling purposes, some compression test samples are fabricated too. All the samples are tested in mechanical compression and their stress–strain response is obtained. Considering the amount of layer penetration, a parametric finite element model is developed to simulate the mechanical properties of the bone scaffolds. The elastic modulus obtained numerically is compared with the experimentally measured one and a good agreement is observed. Moreover, the effects of struts' diameter and layer penetration on the elastic modulus of the bone scaffolds are investigated. Finally, the effect of post-heating is studied and experimental results are compared with the outcomes of the proposed finite element model.

2. Materials and methods

In this section, first of all, the fabrication process of the bone scaffold is presented. Then, the mechanical compression test is briefly reviewed. Finally, the proposed finite element model is presented.

2.1. *Fabrication of scaffolds*

As mentioned before, fabrication of bone scaffolds is performed based on parameters reported in other researches. One of the most important biological features which should be taken into account is the pore size of the bone scaffolds (Annabi et al., 2009; Cicuéndez et al., 2012; Sondergaard et al., 2012; Zimmermann et al., 2008). The appropriate range of porosity for bone regeneration was determined through experimental investigations of biomaterials (Yang et al., 2001). Zein et al. (2002) suggested that bone scaffolds' pore size should be in the range of 160–700 μm. A library for the structure of bone scaffolds produced via additive manufacturing was reported by Cheah et al. (2003a, 2003b).

In this study, all the scaffolds are designed with the pore size and struts' diameter of 350 and 700 μm, respectively. For this purpose, a G-Code program is developed so that it contains all the considerable parameters like the amount of struts' diameter and pore size. This G-code data will then be used as the input of FDM machine.

Poly lactic acid (PLA), a biocompatible and biodegradable polymer, supplied by Shenzhen Esun Industrial Company (natural grade) is used for the fabrication of bone scaffolds. Some properties of the PLA polymer filaments applied in the fabrication process are shown in Table 1.

RAPMAN 3.2 supplied by Bits from Bytes (Clevedon, UK) with two nozzle head is used for the fabrication of scaffolds as well as compression test samples. Referring to Table 1, the nozzle temperature and layer thickness are adjusted to be about 195 °C and 0.5 mm, respectively. Fig. 2 shows one porous bone scaffold fabricated by FDM machine.

Table 1 – Properties of the applied PLA for bone scaffold fabrication.

T_g(°C)	62
T_c(°C)	112
T_m(°C)	170

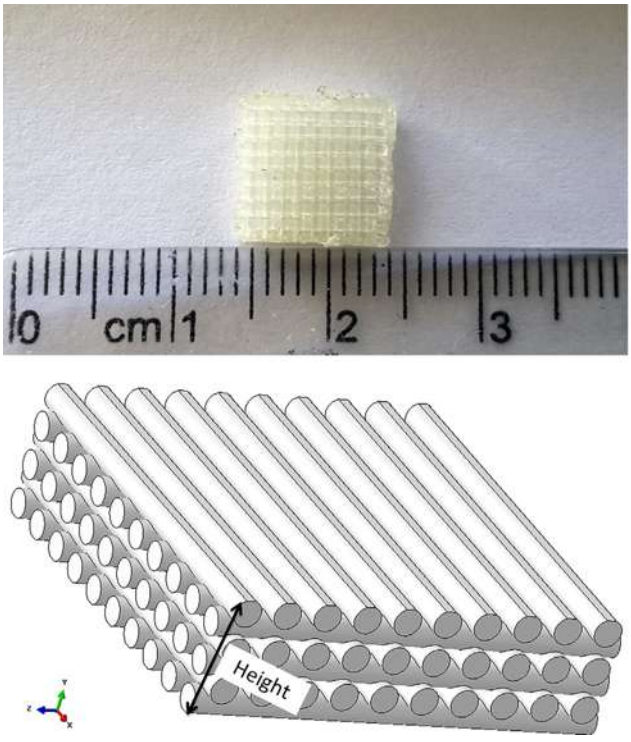

Fig. 2 – (a) Front view of the fabricated bone scaffold via FDM technique and (b) three dimensional view of the designed scaffold.

2.2. Characterization

2.2.1. Compression tests

Since the bone scaffolds are used as bone implants, their compressive mechanical response is of importance. To assess the compressive response of the fabricated bone scaffolds, specimens are prepared based on ISO 604/B1 standard (ISO 604:2002, 2002). According to this standard, samples are cut from larger blocks into $10 \times 10 \times 3\,mm^3$ and tests are carried out with a velocity of 1 mm/min (strain rate of approximately $42 \times 10^{-4}\,S^{-1}$) and a preload of 1.5 N. All the compression tests are performed on HOUNSFIELD (H50KS) (Shakopee, USA). Fig. 3 demonstrates the setup of compression tests. It is necessary to obtain the mechanical response of the bulk material for modeling purposes. To do so, some cylindrical compression test samples are fabricated and tested according to ASTM D 695 standard (ASTM: D 695 – 02a, 2002). The strain rate utilized for these compression tests is about $10^{-4}\,s^{-1}$.

2.2.2. Microscopic images

To be able to characterize the microstructure of the fabricated scaffolds, some microscopic images are taken. All these images are captured by the versatile digital microscope (Dino-Lite Company, Netherlands) with 50 times magnification. The height of the microscope is changed in order to achieve an appropriate quality.

2.3. Finite element model

For predicting the mechanical behavior of the fabricated bone scaffolds, a python script is developed to generate parametric finite element model through the finite element package ABAQUS 6.11-1. In this section, this finite element model is presented in details.

As shown in Fig. 4, the finite element model is constructed by repeating some cylinders with the diameter of D in X, Y, and Z directions. The axis of the cylinders of each layer is perpendicular to that of its upper and lower layers. N_x is the number of cylinders in x direction, N_z the number of cylinders in z direction, N_{yx} the number of cylinders parallel to x in y direction, and N_{yz} the number of cylinders parallel to z direction in y direction. The cylinder of a layer is penetrated to those of its upper and lower one. This value is defined with δ_m as the amount of inter-layer penetration. The distance between two neighbor cylinders in the layers parallel to X and Z axis can be different which are indicated by parameters R_x and R_z, respectively. Moreover, P_x and P_z are defined as the amount of extra material exceeding from the main borders of scaffold in x and z direction, respectively. To be able to model the uniaxial compression test, the upper and lower layers of the bone scaffold is cut with the value of δ_{end}. It is worth mentioning that the effect of shrinkage is not included in the developed model. However, it is possible to modify the model's dimensions according to the microscopic images to take this factor into account. Note that as PLA utilized for fabrication in this research, the effect of shrinkage is not significant because PLA has low shrinkage rather than materials like ABS (Cerdà et al., 2015).

To be coincided with the compression test, all the translational degree of freedoms of the lower faces of the scaffold are fixed, while for the upper faces, the translational degrees of freedom perpendicular to the loading direction are fixed and that parallel to the loading direction is moved toward the lower face with the value of compression displacement (Δ) as shown in Fig. 5.

According to what mentioned above, the geometry of the finite element model can be described using D, R_x, R_z, P_x, P_z, δ_m, δ_{end}, N_x, N_{yx}, N_{yz}, *and* N_z parameters. Referring to the model, the bone scaffold's dimension in x, y, and z directions can be calculated using the following equations respectively.

$$L_x = 2P_x + N_xD + (N_x - 1)R_x \quad (1)$$

$$L_z = 2P_z + N_zD + (N_z - 1)R_z \quad (2)$$

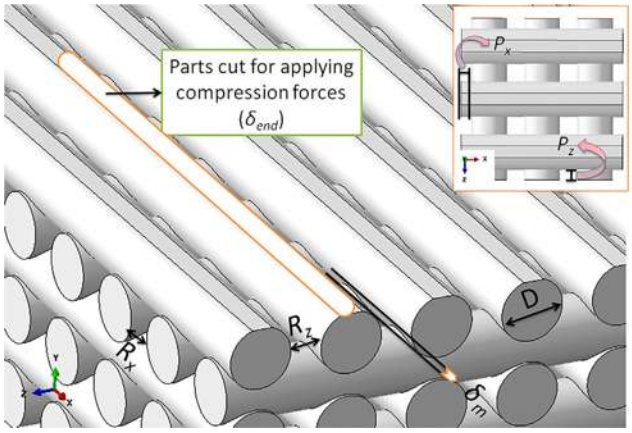

Fig. 4 – Schematic of the internal structure and parameters of the designed scaffold in finite element model.

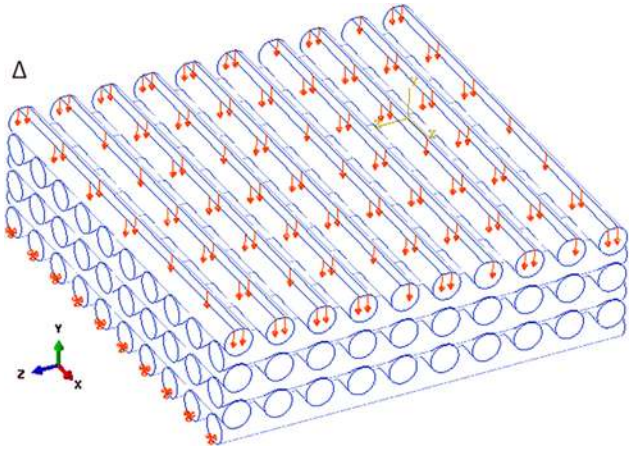

Fig. 5 – Schematic of the applied boundary conditions to the bone scaffold.

Fig. 3 – View of the performed compression tests setup.

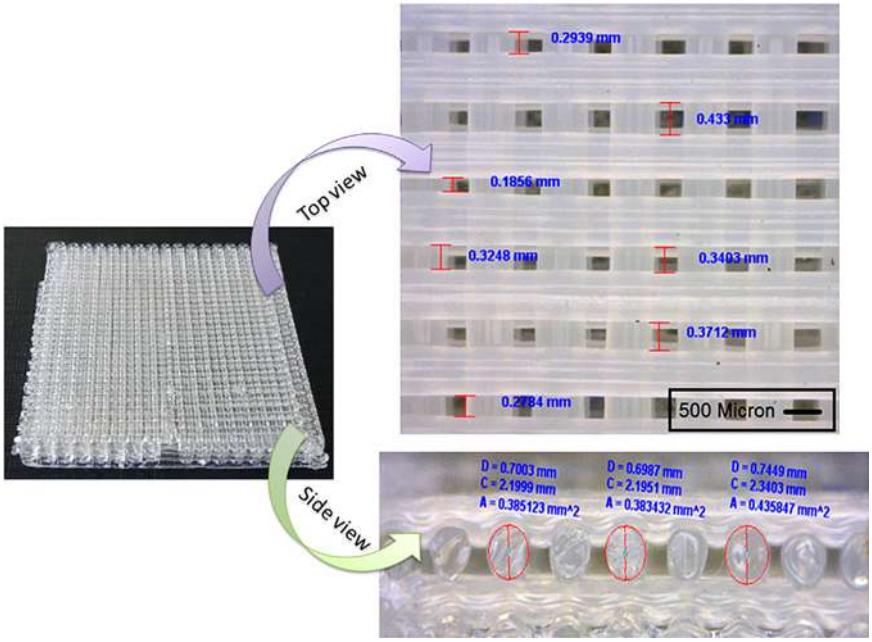

Fig. 6 – The microscopic view of the fabricated scaffold.

$$L_y = \begin{cases} 2\left(\frac{D}{2} - \delta_{end} + N_{yz}(D-\delta_m)\right) & N_{yz} = N_{yx} - 1 \\ 2\left(\frac{D}{2} - \delta_{end} + N_{yz}(D-\delta_m)\right) - (D-\delta_m) & N_{yz} = N_{yx} \end{cases} \quad (3)$$

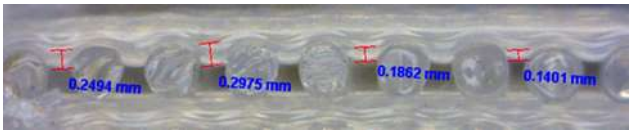

Fig. 7 – The amount of layer penetration between additive manufactured bone scaffold layers.

3. Results

In the following section, first, the microstucture of the fabricated bone scaffolds as well as their compressive mechanical response is presented. Then, the results of finite element simulations are discussed.

3.1. *Experiment*

Fig. 6 shows one fabricated bone scaffold and its microscopic images. Using the microscopic images, the pore size and struts' diameter measured to be 0.7 ± 0.12 and 0.35 ± 0.08 mm, respectively. As it can be seen, the average value of these two parameters is nearly equal to that defined in the G-code. Also, the amount of scaffold's porosity is measured by Archimedes principle which is about 40%.

Fig. 7 shows a side view microscopic image of the fabricated bone scaffold. Referring to this figure, the layer penetration value is measured to be 0.22 ± 0.06 mm.

Fig. 8a and b depicts the stress–strain curve of the bulk compression specimen and the bone scaffold. As it can be seen, there is a nonlinear region at the initial portion of the curve called “toe region”. This nonlinear region makes the calculation of elastic modulus difficult. Accordingly, the method presented in ASTM: D 695 – 02a (2002) is utilized here for the calculation of the elastic modulus. To do so, continuation of the linear region of the curve is intersected by the zero-stress axis. This intersection shown by ε_0 is regard as the corrected zero strain point from which all strains must be measured. Using this method the elastic modulus of the bulk material and bone scaffold is calculated to be 1517.85 ± 17.45 MPa and 183.62 ± 22.85 MPa respectively.

3.2. *Finite element model*

The geometrical parameters obtained from microscopic images are used to generate the finite element model. Table 2 shows the geometrical parameters used for the present simulations. In addition, the value of loading parameter, Δ, is supposed to be 0.2 mm. Using these geometrical parameters the dimensions of the bone scaffold is calculated to be about 10.17, 3.06, and 10.17 mm in x, y, and z directions, respectively.

All the simulations are performed on 2.93 GHz processors with 24 cores and 24 GB RAM provided by National High-Performance Computing Center of Isfahan University of Technology. The model is meshed using 10-node modified quadratic tetrahedron elements with four integration points denoted by C3D10 in ABAQUS. Fig. 9 shows the meshed configuration of the model.

As shown in Fig. 10, a mesh sensitivity analysis is conducted by repeatedly reducing the mesh size and rerunning the analysis until changes in the results are negligible. Using this method, the value of 0.6 is obtained for the mesh size and used for all the simulations.

The numerically calculated elastic modulus of the bone scaffold is about 213.21 MPa which is about 16.11% higher than that obtained experimentally. This difference can be due

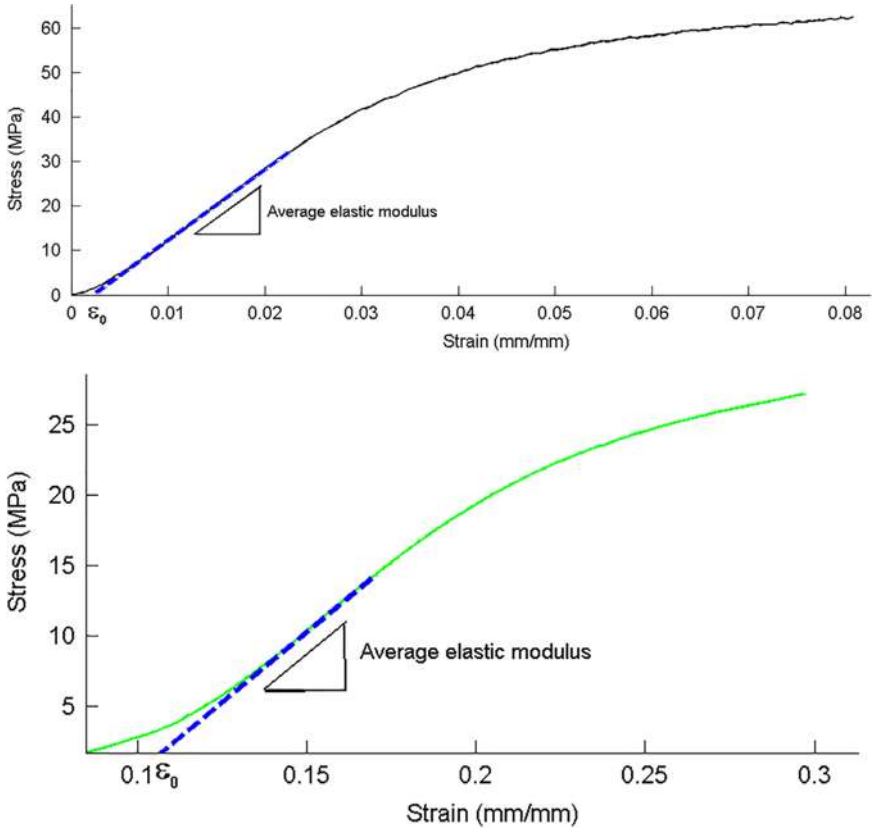

Fig. 8 – Experimental and corrected stress–strain curve of (a) the bulk material and (b) the bone scaffold specimen.

Table 2 – Geometrical parameters utilized in finite element model.

Parameter	Determined value (mm)
D	0.70
R_x, R_z	0.35
δ_m	0.22
δ_{end}	0.02
N_x	10
N_y	3
Nz	10

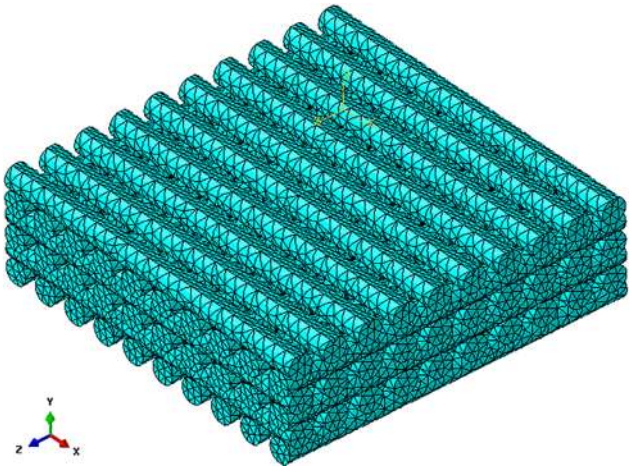

Fig. 9 – A schematic of the meshed bone scaffold.

to the existence of some microstructural defects in the microstructure of the scaffold. Karamooz Ravari and Kadkhodaei (2015) and Karamooz Ravari et al. (2015a, 2015b, 2014) showed that the microstructural imperfections can severely affect the mechanical response of porous materials as well as cellular lattice structures.

4. Discussions

In this section, first, the effects of geometrical parameters including struts' diameter and layer penetration on the elastic modulus of the bone scaffold are investigated using finite element approach. Finally, the effect of post-heating on the elastic modulus of fabricated bone scaffolds as well as compression test samples is assessed through experimental and numerical investigations.

4.1. *Effects of the geometrical parameters on the elastic modulus of bone scaffold*

Fig. 11 shows the elastic modulus of the bone scaffold for three different values of struts' diameter. According to this figure, the elastic modulus increases by increasing the value of struts' diameter as a result of lower porosity. Although increase the amount of strut diameter enhances the bone scaffold elastic modulus, its biological features such as pore size will be affected. In a fixed value of porosity, increasing

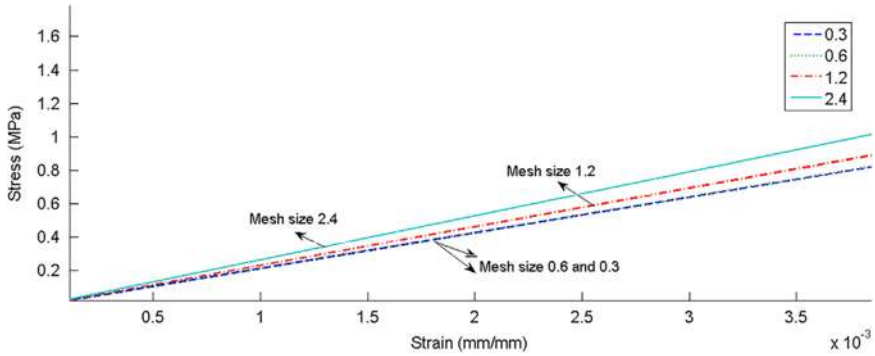

Fig. 10 – The results of mesh sensitivity analysis.

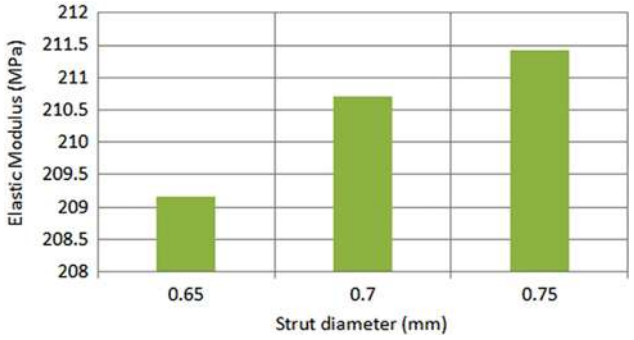

Fig. 11 – Investigation of the effect of struts' diameter on the elastic modulus of bone scaffold.

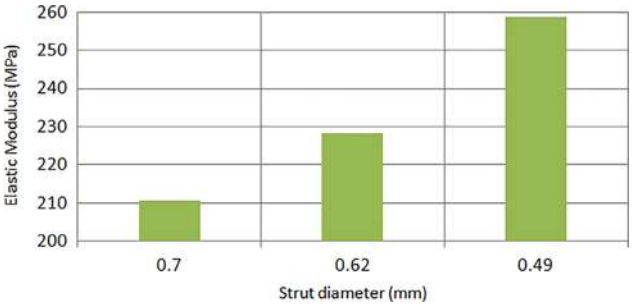

Fig. 12 – Investigation of the effect of struts' diameter on mechanical properties in fix porosity.

the amount of strut diameter (by having low numbers of wider ligaments) leads to restricted conditions for transporting nutrition because of a considerable decrease in pore size. This is where that the importance of being a balance between mechanical and biological properties shows itself.

Additionally, strut diameter affects the amount of fusion which has an inevitable effect on the mechanical properties of bone scaffolds. Numerous studies were reported on the bone scaffolds fabricated by melt electrospinning with smaller strut diameter rather than FDM technique (Hutmacher and Dalton, 2011; Visser et al., 2015). While in methods like FDM the strut diameter is restricted to be greater than 100 μm, melt electrospinning makes it possible to obtain smaller diameters (Brown et al., 2011). To evaluate the effects of strut diameter on the mechanical properties of bone sccafolds, three groups of scaffolds are investigated with similar value of porosity (about 40%), but different diameters of 0.49, 0.62 and 0.7 mm. Note that to be able to fix the value of porosity, it is necessary to change the number of struts as well as their distance. As it is shown in Fig. 12, at a fix value of porosity, the smaller strut diameter results in higher elastic modulus. Thus, it is necessary to choose the method of fabrication based on the desired mechanical and geometrical properties.

The effect of layer penetration on the elastic modulus of the fabricated bone scaffolds is shown in Fig. 13. It can be concluded from this figure that there is a direct correlation between layer penetration and elastic modulus. The elastic modulus increases almost linearly by the value of layer penetration.

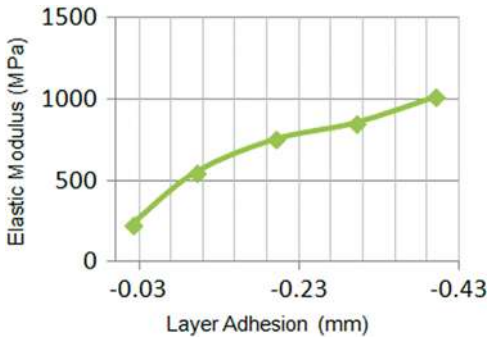

Fig. 13 – Effect of layer penetration on the elastic modulus of bone scaffold.

4.2. *Investigation of post-heating effect on the elastic modulus*

To achieve desirable futures of a fabricated part, post-heating of those parts may be applied. In this study, some scaffolds with the struts' diameter of 700 and pore size of 350 μm are heated up to 3 °C more than crystallization temperature of the PLA which is about 115 °C. They are kept for 300 s at this temperature and then cooled down to the room temperature. Fig. 14a and b shows the average compressive stress–strain response of the bulk material and post-heated scaffolds respectively. Using the method presented in Section 3.1, the average elastic modulus of the bone scaffold and the compression test specimens is obtained to be 210.29±19.20 MPa and 1576.20±24.58 MPa respectively. It is worth mentioning

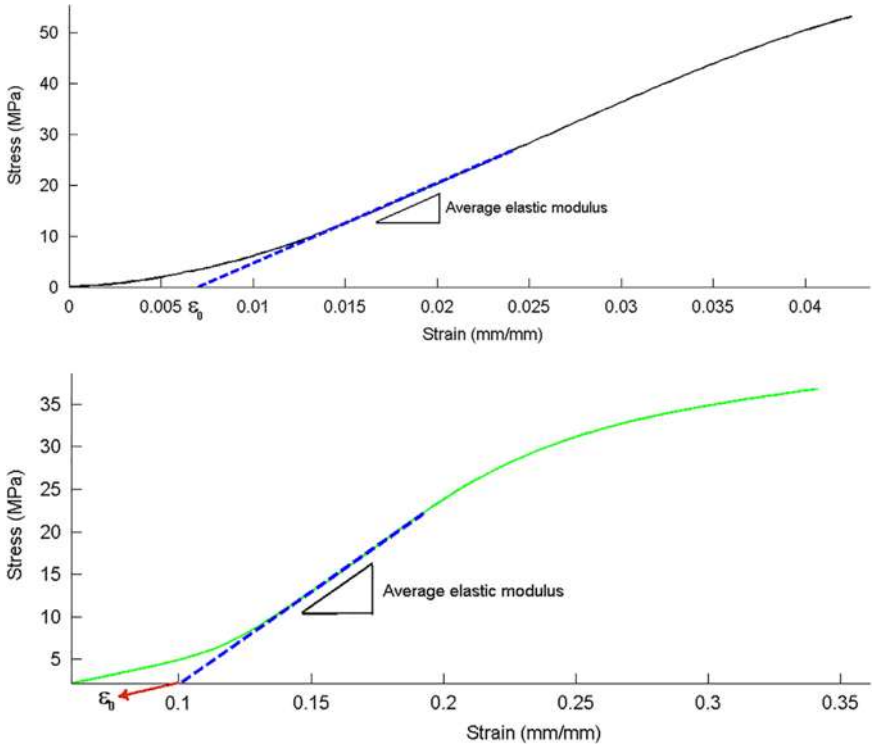

Fig. 14 – Experimental and corrected stress–strain curve of (a) the bulk post-heated and (b) post-heated bone scaffold specimen.

that all the compression tests of both scaffold and bulk material are performed similar to the as-built ones.

As it can be seen, the elastic modulus of the post-heated scaffold as well as bulk sample is higher than that of the as-built samples. It can be justified in such a way that by holding the samples at a sufficiently high temperature for a reasonably enough time, the layers of the material stick to each other more than the layers of the as-built samples. In other words, this increase is due to higher amount of inter-layer bonding of solidified struts. Accordingly, a more uniform material distribution is obtained causing higher stress level in the stress–strain curve in a specific value of strain. In addition, there might be some micro-pores in the structure of the as-built samples which would be filled after post-heating of the samples which lead to more pronounced mechanical properties. Beyond the effect of layer penetration on the mechanical properties of the FDM parts, this factor may affect tribological behavior of them as a paramount factor, which plays a decisive role in their friction coefficient and friction force. It was reported that the wear mechanism of the FDM parts fabricated by ABS is according to de-lamination (Boparai et al., 2015). Consequently, in general, post-heating may increase inter-layer bonding which could enhance tribological properties of FDM parts, e.g. greater wear resistance and lower friction coefficient. In addition, control of accuracy and precision is really important in FDM parts. Berger (2015) reported the aspects of accuracy in the additive manufactured plastic gears. Although increasing the layer penetration by post-heating may improve the mechanical response, it can decrease the dimensional accuracy.

The numerically calculated elastic modulus of the bone scaffold is about 210.32 MPa which is 0.02% higher than that obtained experimentally. It shows that developed model could predict the elastic modulus of post-heated bone scaffolds more accurately in comparison with as-built ones. Due to strict adhesion of layers and existence of fewer pores in the post-heated bulk samples, their stress–strain response is more accurate in comparison with that of the as-built samples. In addition, the layers of the as-built bone scaffolds are more defected than those of the post-heated samples. However, the effects of these defects are not taken into account in the finite element model. According to what mentioned above, the predictions of the model are more accurate for the post-heated samples.

5. Conclusions

The main goal of the present study is to investigate the mechanical response of polymeric bone scaffolds fabricated by fused deposition modeling. To do so, some bone scaffolds are designed and fabricated using suitable geometrical parameters. To be able to characterize the bulk material of the bone scaffolds, some compression test specimens are also fabricated. All the specimens are tested in compression and their elastic modulus is obtained. Using the material parameters of the compression test samples as the bulk material of the bone scaffold, a parametric finite element model is also developed to predict the elastic response of the bone scaffolds. The obtained numerical elastic modulus is compared with the experimentally measured one showing a good agreement. In

addition, the effect of layer penetration which is inseparable part of additive manufactured parts is investigated. The results show that by increasing the value of layer adhesion, the elastic modulus increases significantly. Finally, the effect of post-heating of bone scaffold as well as compression test samples on their mechanical response is investigated. The results show that post-heating of both bone scaffold and compression test sample increases the value of their elastic modulus. The numerically obtained elastic modulus is about 213.21 MPa and 210.32 MPa for as-built and post-heated scaffolds respectively. These values are about 16.11% and 0.02% higher than the corresponding experimentally measured value. Based on the achieved outcomes, presented finite element model is an efficient numerical model for the investigation of the mechanical response of the bone scaffolds fabricated by FDM technique, especially post-heated ones.

Acknowledgment

The authors would like to thank National High-Performance Computing Center of Isfahan University of Technology. All the simulations are performed in this center.

REFERENCES

Ang, K.C., Leong, K.F., Chua, C.K., Chandrasekaran, M., 2007. Compressive properties and degradability of poly(ε-caprolatone)/hydroxyapatite composites under accelerated hydrolytic degradation. J. Biomed. Mater. Res. Part A 80A, 655–660, http://dx.doi.org/10.1002/jbm.a.30996.

Annabi, N., Mithieux, S.M., Boughton, E.A., Ruys, A.J., Weiss, A.S., Dehghani, F., 2009. Synthesis of highly porous crosslinked elastin hydrogels and their interaction with fibroblasts in vitro. Biomaterials 30, 4550–4557.

ASTM: D 695 – 02a, 2002. Standard Test Method For Compressive Properties of Rigid Plastics.

Berger, U., 2015. Aspects of accuracy and precision in the additive manufacturing of plastic gears. Virtual Phys. Prototyp, 1–9.

Boccaccio, A., Ballini, A., Pappalettere, C., Tullo, D., Cantore, S., Desiate, A., 2011. Finite element method (FEM), mechanobiology and biomimetic scaffolds in bone tissue engineering. Int. J. Biol. Sci. 7, 112.

Boparai, K., Singh, R., Singh, H., 2015. Comparison of tribological behaviour for Nylon6–Al–Al_2O_3 and ABS parts fabricated by fused deposition modelling: this paper reports a low cost composite material that is more wear-resistant than conventional ABS. Virtual Phys. Prototyp 10, 59–66.

Brown, T.D., 2000. Techniques for mechanical stimulation of cells in vitro: a review. J. Biomech. 33, 3–14.

Brown, T.D., Dalton, P.D., Hutmacher, D.W., 2011. Direct writing by way of melt electrospinning. Adv. Mater. 23, 5651–5657.

Cerdà, V., Avivar, J., Moreno, D., 2015. Chips: how to build and implement fluidic devices in flow based systems. Talanta, 1–8, http://dx.doi.org/10.1016/j.talanta.2015.11.073.

Cheah, C.M., Chua, C.K., Leong, K.F., Chua, S.W., 2003a. Development of a tissue engineering scaffold structure library for rapid prototyping. Part 2: parametric library and assembly program. Int. J. Adv. Manuf. Technol. 21, 302–312.

Cheah, C.M., Chua, C.K., Leong, K.F., Chua, S.W., 2003b. Development of a tissue engineering scaffold structure library for rapid prototyping. Part 1: investigation and classification. Int. J. Adv. Manuf. Technol. 21, 291–301.

Cicuéndez, M., Izquierdo-Barba, I., Sánchez-Salcedo, S., Vila, M., Vallet-Regí, M., 2012. Biological performance of hydroxyapatite–biopolymer foams: in vitro cell response. Acta Biomater. 8, 802–810.

De Long, W.G., Einhorn, T.A., Koval, K., McKee, M., Smith, W., Sanders, R., Watson, T., 2007. Bone grafts and bone graft substitutes in orthopaedic trauma surgery: a critical analysis. J. Bone Joint Surg. Am. 89, 649–658.

Dias, M.R., Guedes, J.M., Flanagan, C.L., Hollister, S.J., Fernandes, P.R., 2014. Optimization of scaffold design for bone tissue engineering: a computational and experimental study. Med. Eng. Phys. 36, 448–457.

Doyle, H., Lohfeld, S., Dürselen, L., McHugh, P., 2015. Computational modelling of ovine critical-sized tibial defects with implanted scaffolds and prediction of the safety of fixator removal. J. Mech. Behav. Biomed. Mater. 44, 133–146.

Gao, C., Wang, D., Shen, J., 2003. Fabrication of porous collagen/chitosan scaffolds with controlling microstructure for dermal equivalent. Polym. Adv. Technol. 14, 373–379.

Giannitelli, S.M., Accoto, D., Trombetta, M., Rainer, A., 2014. Current trends in the design of scaffolds for computer-aided tissue engineering. Acta Biomater. 10, 580–594.

Gibson, I., Rosen, D., Stucker, B., 2015. Additive Manufacturing Technologies. Springer Science and Business Media, New York.

Godbey, W.T., Atala, A., 2002. In vitro systems for tissue engineering. Ann. N. Y. Acad. Sci. 961, 10–26.

Harris, L.D., Kim, B.-S., Mooney, D.J., 1998. Open Pore Biodegradable Matrices Formed With Gas Foaming.

Hollister, S.J., Lin, C.Y., 2007. Computational design of tissue engineering scaffolds. Comput. Methods Appl. Mech. Eng. 196, 2991–2998.

Hutmacher, D.W., 2000. Scaffolds in tissue engineering bone and cartilage. Biomaterials 21, 2529–2543.

Hutmacher, D.W., Dalton, P.D., 2011. Melt electrospinning. Chem. Asian. J. 6, 44–56.

ISO 604:2002, 2002. Plastics—Determination of Compressive Properties.

Jariwala, S.H., Lewis, G.S., Bushman, Z.J., Adair, J.H., Donahue, H. J., 2015. 3D printing of personalized artificial bone scaffolds. 3D Print. Addit. Manuf. 2, 56–64.

Karamooz Ravari, M.R., Kadkhodaei, M., 2015. A computationally efficient modeling approach for predicting mechanical behavior of cellular lattice structures. J. Mater. Eng. Perform. 24 (1), 245–252.

Karamooz Ravari, M.R., Kadkhodaei, M., 2013. Finite element modeling of the elastic modulus of Ti6al4v scaffold fabricated by SLM, In: Proceedings of the Fifth Biot Conference On Poromechanics V5, pp. 1021–1028.

Karamooz Ravari, M.R., Kadkhodaei, M., Badrossamay, M., Rezaei, R., 2014. Numerical investigation on mechanical properties of cellular lattice structures fabricated by fused deposition modeling. Int. J. Mech. Sci. 88, 154–161.

Karamooz Ravari, M.R., Kadkhodaei, M., Ghaei, A., 2015a. A unit cell model for simulating the stress–strain response of porous shape memory alloys. J. Mater. Eng. Perform. 24 (10), 4096–4105.

Karamooz Ravari, M.R., Kadkhodaei, M., Ghaei, A., 2015b. Effects of asymmetric material response on the mechanical behavior of porous shape memory alloys. J. Intell. Mater. Syst. Struct. http://dxdoi.org/10.1177/1045389X15604232.

Laurent, C.P., Latil, P., Durville, D., Rahouadj, R., Geindreau, C., Orgéas, L., Ganghoffer, J.-F., 2014. Mechanical behaviour of a fibrous scaffold for ligament tissue engineering: finite elements analysis vs. X-ray tomography imaging. J. Mech. Behav. Biomed. Mater. 40, 222–233.

Liu, P.F., Zheng, J.Y., 2010. Recent developments on damage modeling and finite element analysis for composite laminates: a review. Mater. Des. 31, 3825–3834.

Martínez, J., Diéguez, J.L., Ares, E., Pereira, A., Hernández, P., Pérez, J.A., 2013. Comparative between FEM models for FDM parts and their approach to a real mechanical behaviour. Procedia Eng. 63, 878–884.

Mikos, A.G., Sarakinos, G., Leite, S.M., Vacant, J.P., Langer, R., 1993. Laminated three-dimensional biodegradable foams for use in tissue engineering. Biomaterials 14, 323–330.

Moroni, L., De Wijn, J.R., Van Blitterswijk, C.A., 2006. 3D fiber-deposited scaffolds for tissue engineering: influence of pores geometry and architecture on dynamic mechanical properties. Biomaterials 27, 974–985.

Mullender, M., El Haj, A.J., Yang, Y., Van Duin, M.A., Burger, E.H., Klein-Nulend, J., 2004. Mechanotransduction of bone cells in vitro: mechanobiology of bone tissue. Med. Biol. Eng. Comput. 42, 14–21.

Poh, S.P.P., 2014. In Vitro and In Vivo Assessment of Bioactive Composite Scaffolds Fabricated Via Additive Manufacturing Technology. Queensland University of Technology, Australia.

Sahai, N., Jain, T., Kumar, S., Dutta, P.K., 2016. Development and Selection of Porous Scaffolds Using Computer-Aided Tissue Engineering. http://dx.doi.org/10.1007/978-81-322-2511-9.

Sanz-Herrera, J.A., Kasper, C., van Griensven, M., Garcia-Aznar, J. M., Ochoa, I., Doblare, M., 2008. Mechanical and flow characterization of Sponceram® carriers: evaluation by homogenization theory and experimental validation. J. Biomed. Mater. Res. Part. B: Appl. Biomater. 87, 42–48.

Scaffaro, R., Lopresti, F., Botta, L., Rigogliuso, S., Ghersi, G., 2016. Preparation of three-layered porous PLA/PEG scaffold: relationship between morphology, mechanical behavior and cell permeability. J. Mech. Behav. Biomed. Mater. 54, 8–20.

Singh, B.K., Sirohi, R., Archana, D., Jain, A., Dutta, P.K., 2015. Porous chitosan scaffolds: a systematic study for choice of crosslinker and growth factor incorporation. Int. J. Polym. Mater. Polym. Biomater. 64, 242–252.

Sondergaard, C.S., Witt, R., Mathews, G., Najibi, S., Le, L., Clift, T., Si, M.-S., 2012. Prevascularization of self-organizing engineered heart tissue by human umbilical vein endothelial cells abrogates contractile performance. Cell Tissue Res. 350, 439–444.

Sudarmadji, N., Tan, J.Y., Leong, K.F., Chua, C.K., Loh, Y.T., 2011. Investigation of the mechanical properties and porosity relationships in selective laser-sintered polyhedral for functionally graded scaffolds. Acta Biomater. 7, 530–537, http://dx.doi.org/10.1016/j.actbio.2010.09.024.

Thomson, R.C., Wake, M.C., Yaszemski, M.J., Mikos, A.G., 1995. Biodegradable polymer scaffolds to regenerate organs. In: Prof. Nicholas A. Peppas, Prof. Robert S. Langer (Eds.), Biopolymers II, Springer, Berlin, Heidelberg, Germany, pp. 245–274.

Visser, J., Melchels, F.P.W., Jeon, J.E., van Bussel, E.M., Kimpton, L. S., Byrne, H.M., Dhert, W.J.A., Dalton, P.D., Hutmacher, D.W., Malda, J., 2015. Reinforcement of hydrogels using three-dimensionally printed microfibres. Nat. Commun. 6, 1–10.

Whang, K., Thomas, C.H., Healy, K.E., Nuber, G., 1995. A novel method to fabricate bioabsorbable scaffolds. Polymer 36, 837–842.

Widmer, M.S., Mikos, A.G., 1998. Fabrication of Biodegradable Polymer Scaffolds for Tissue Engineering. Elsevier Sciences, New York.

Wieding, J., Wolf, A., Bader, R., 2014. Numerical optimization of open-porous bone scaffold structures to match the elastic properties of human cortical bone. J. Mech. Behav. Biomed. Mater. 37, 56–68.

Yang, S., Leong, K.-F., Du, Z., Chua, C.-K., 2001. The design of scaffolds for use in tissue engineering Part I. Traditional factors. Tissue Eng. 7, 679–689.

Zein, I., Hutmacher, D.W., Tan, K.C., Teoh, S.H., 2002. Fused deposition modeling of novel scaffold architectures for tissue engineering applications. Biomaterials 23, 1169–1185, http://dx.doi.org/10.1016/S0142-9612(01)00232-0.

Zhou, Q., Gong, Y., Gao, C., 2005. Microstructure and mechanical properties of poly (L-lactide) scaffolds fabricated by gelatin particle leaching method. J. Appl. Polym. Sci. 98, 1373–1379.

Zimmermann, M., Flechsig, C., La Monica, N., Tripodi, M., Adler, G., Dikopoulos, N., 2008. Hepatitis C virus core protein impairs in vitro priming of specific T cell responses by dendritic cells and hepatocytes. J. Hepatol. 48, 51–60.